International Journal of Trend in Research and Development, Volume 13(3), ISSN: 2394-9333
www.ijtrd.com

Construction and Performance of Pt/MoB Electrocatalyst for HER

Wu Yifan
School of Materials Science and Engineering, Henan Polytechnic University, Jiaozuo, China

Abstract**—**This work reports the preparation of a Pt/MoB electrocatalyst for hydrogen evolution reaction (HER) in acidic media via a facile etching and reduction method. MoB MBene was successfully synthesized by etching MoAlB with hydrofluoric acid, followed by loading Pt nanoparticles through chemical reduction. Structural characterizations confirm the layered morphology of MoB and uniform dispersion of metallic Pt on the support, with a strong metal-support interaction between Pt and MoB. Electrochemical tests in 0.5 M H_2SO_4 show that Pt/MoB exhibits overpotential of 69 mV at −10 mA·cm^{-2} and Tafel slope of 27 mV·dec^{-1}, with activity comparable to Pt/Mo_2C. The catalyst also displays excellent stability after 1000 CV cycles and 3000 s chronoamperometry measurement. This study demonstrates that MoB is a promising support for Pt-based electrocatalysts, providing a new strategy for designing efficient and stable HER catalysts.

Keywords**—***Hydrogen evolution reaction; Pt/MoB electrocatalyst; Metal-support interaction; Electrochemical stability; Molybdenum boride*

I. INTRODUCTION

It is urgent to develop renewable and sustainable energy because of the energy shortage, greenhouse effect and environmental pollution[1]. Hydrogen is largely recognized as a cost-efficient clean fuel[9]. Relative to traditional technologies, the electrocatalytic overall water-splitting is widely regarded as an efficient avenue to generate hydrogen[16]. Hitherto, platinum and other precious metals are the first choice for hydrogen evolution reaction (HER) eletrocatalysts.However, the high cost and low reserves of Pt-based electrocatalysts restricts their application[19]. Therefore, it is essential to explore.

In recent years, molybdenum-based materials, such as molybdenum disulfide[23], molybdenum carbide[25], and molybdenum phosphide[27], have been widely studied as low-cost electrocatalysts. Metal borides have garnered significant attention for their exceptional properties and varied structures[29]. In particular, molybdenum borides own good electrical conductivity and abundant catalytic active sites. This is attributed to the electron deficiency present in boron atoms [31]. The deficiency of electrons leads boron atoms to form more complex covalent bonds with other elements[32]. Among them, molybdenum boride (MoB) is an emerging member of the MBene family. Its catalytic performance has not been fully investigated, and it features simpler preparation processes and lower costs. Therefore, high catalytic activity is expected to achieve by dispersing precious metals onto the MoB substrate.

In this work, platinum was loaded on MoB substrates. The hydrogen evolution performance of the as-prepared catalyst was tested and compared. The MoB substrate significantly improved the dispersion of Pt sites, fully exposed the active sites, and enhanced the electrochemical hydrogen evolution performance. The prepared Pt/MoB catalyst exhibited excellent hydrogen evolution activity. Furthermore, its overall performance is comparable to that of the well-developed Mo_2 C catalyst, demonstrating its great potential for further research.

II. METHOD

In this experiment, MoAlB is prepared in the first step.the specific steps are as follows: First, MoAlB was synthesized using MoB powder (>99%, Energy Chemical, Anhui, China) and Al powder (>99.5%, 200 mesh, Bike New Material Technology, Shanghai, China) as starting materials. MoB and Al powders with a molar ratio of 1:1.3 were ball-milled in a glass container for 12 h to ensure thorough mixing. To guarantee uniform reaction at high temperature, the mixed powder was pressed into a circular disk under 20 MPa for 5 min using a cold press. After cold pressing, the circular disk was heated at 1200 °C for 5 h in a tube furnace under an argon atmosphere. After the sample cooled naturally to room temperature, it was ground into powder using a mortar and pestle and sieved through a 500-mesh sieve. Subsequently, the obtained MoAlB powder was immersed in 2 M HCl solution under stirring for 24 h. After the reaction, the powder was centrifugally washed with deionized water and finally vacuum-dried at 60 °C for 12 h to obtain pretreated MoAlB powder.

In this experiment, MoAlB is prepared first, followed by the synthesis of MoB.at room temperature, 40 mL of 40% hydrofluoric acid (HF) solution was placed in a polytetrafluoroethylene beaker. 1 g of sieved MoAlB powder was slowly added to the beaker in portions, followed by ultrasonication for 30 min to ensure uniform dispersion of MoAlB powder in the HF solution (this step must be carried out in a fume hood with proper safety protection). The mixture was then sealed in a 100 mL autoclave and heated in an oven at 160 °C for 24 h. After the reaction completed and the system cooled naturally, the solution in the autoclave was transferred to centrifuge tubes and washed with deionized water and ethanol alternately via multiple centrifugations until the supernatant was neutral. Due to the difference in specific mass between MoB and the generated fluoride by-products, MoB MBene powder deposited at the bottom of the centrifuge tube. The precipitate was collected and dried in a vacuum oven at 60 °C for 12 h to obtain dry MoB MBene powder, which was then stored in an inert atmosphere for later use.

Finally, Pt is loaded onto MoB.first, 20 mg of MoB was weighed into a beaker, and 20 mL of deionized water was added using a graduated cylinder. The mixture was ultrasonicated for 30 min to uniformly disperse MoB and form a stable black suspension. Subsequently, 0.256 mL of 0.1 mol·L^{-1} K_2 $PtCl_4$ solution was added to the suspension, followed by magnetic stirring for 30 min to ensure uniform dispersion of Pt ions in the system. Finally, 5 mL of $NaBH_4$

solution (1 mg·mL^{-1}) was added to the suspension, and the mixture was stirred continuously for 24 h for reduction. After the reaction, the product was centrifugally washed with deionized water until neutral, and then freeze-dried at -50 °C to obtain the Pt-loaded MoB (Pt/MoB) catalyst. The same preparation method was used to prepare the reference sample Pt/Mo_2 C (20 wt.% Pt) catalyst; the commercial carbon-supported platinum catalyst Pt/C (20 wt.% Pt) was used as received.

III. REAULT & DISCUSSION

A. Microstructure Characterizations

The XRD patterns of MoAlB and MoB are shown in Figure 1. It can be clearly observed that the diffraction peaks of MoAlB at 13°, 25°, 28°, 31°, 39°, 41°, 43°, and 45° correspond to the (020), (040), (110), (021), (060), (111), (150), and (131) crystal planes, respectively. These peaks are highly consistent with its standard reference pattern (PDF #72-1277), with no obvious impurity peaks, indicating the successful synthesis of high-purity MAB-phase MoAlB.after HF treatment, the (040), (111), and (131) peaks of MoAlB at 2θ = 25°, 41°, and 45° disappear significantly. Meanwhile, the diffraction peaks corresponding to the (110) and (021) planes at 28° and 30°, as well as the (006) and (150) planes in the range of 35–45°, are obviously broadened. This is attributed to the loss of crystallinity under aggressive reaction conditions. After etching, the (020) peak of MoAlB at 12.6° completely disappears, and a new peak belonging to the MoB MBene appears at 7.9°, with a significantly increased full width at half maximum (FWHM). These results indicate that the periodicity of the layered structure of MoAlB has been destroyed, and it has been successfully transformed into two-dimensional MoB MBene, realizing the effective and selective removal of the Al atomic layer. This confirms the successful conversion of MoAlB to MoB MBene.

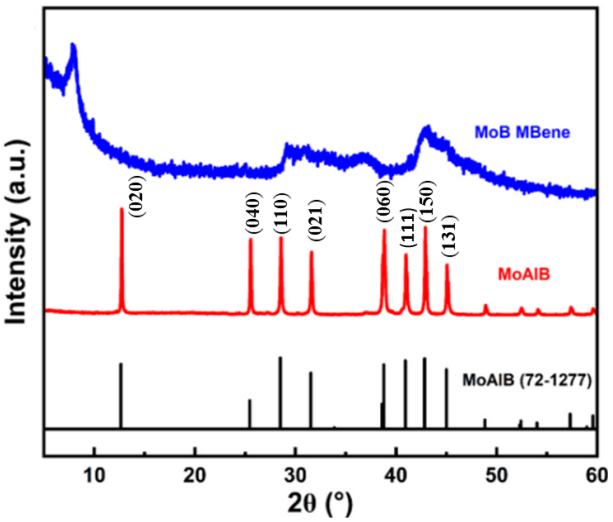

Figure 1. XRD patterns of MoAlB and MoB

The morphologies of the precursor MoAlB and the etched product were observed via field-emission scanning electron microscopy (FE-SEM), as shown in Figure 2. Figure 2(a) shows the precursor MAB-phase MoAlB, which exhibits the typical ternary layered stacking structure of the MAB phase with clear edges and a highly ordered layered structure, serving as an ideal precursor for the successful etching of two-dimensional MoB. Figure 2(b) presents the SEM image of the etched product, which displays the typical accordion-like structure of MBene. This phenomenon is related to the functionalization of the exposed Mo surface after the removal of the Al atomic layer via HF treatment. Specifically, after the delamination of the Al atomic layer, highly active Mo atoms on the MoB surface are exposed and further react with functional groups such as fluoride ions and hydroxyl groups in the reaction solution. Terminal groups including -F and -OH replace the Al atomic layer, functionalizing the surface and thus increasing the interlayer spacing of the sheets. The SEM results also confirm the successful etching of the Al atomic layer, the transformation of MoAlB into MoB MBene, and the structural integrity of the Mo-B layers, verifying the effective etching by HF.

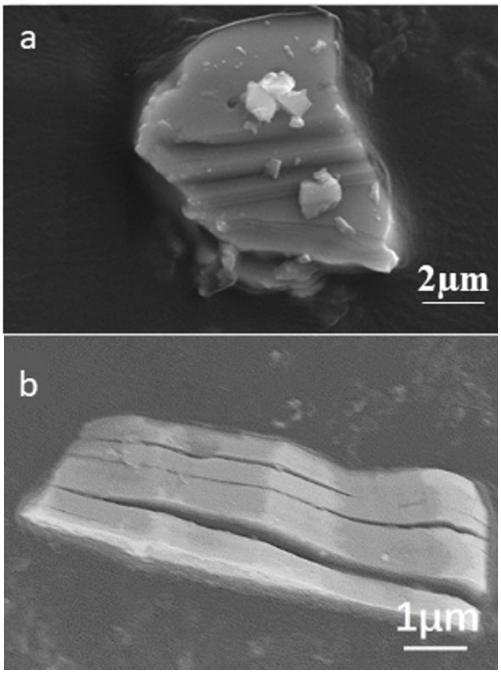

Figure 2. SEM of MoAlB and MoB

The crystal structure and phase composition of the Pt/MoB catalyst were characterized by X-ray diffraction (XRD). As shown in Figure 3(a), several new diffraction peaks appear at approximately 39.9°, 46.5°, and 68.4° in addition to the original XRD pattern of MoB MBene. These peaks match the (111), (200), and (220) crystal planes of face-centered cubic (fcc) Pt nanocrystals (PDF #87-0640), indicating that the Pt loaded on the composite support exhibits high crystallinity. Compared with Figure 3-1, the MoB diffraction peak at 7.9° shows a narrower full width at half maximum (FWHM), which suggests that the oxygen-containing functional groups on the support surface are also reduced during Pt reloading. The coexistence of Pt and MoB diffraction peaks confirms the successful formation of the ternary composite.

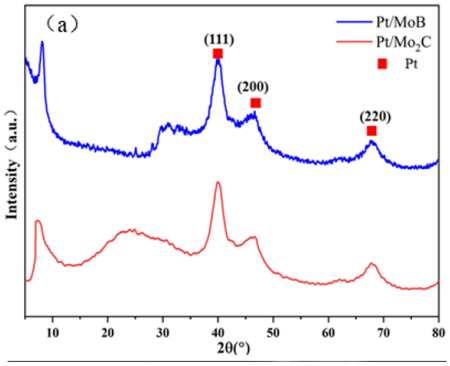

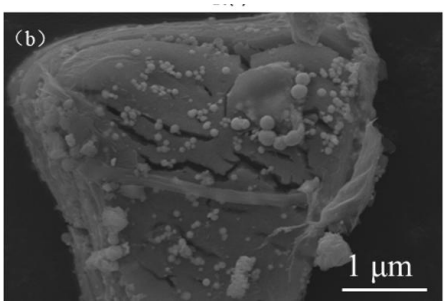

Figure 3. (a) XRD Patterns of Pt/MoB and Pt/Mo_2 C, and (b) SEM Image of Pt/MoB

Figure 3(b) presents the scanning electron microscopy (SEM) morphology characterization of the Pt/MoB composite catalyst. The MoB support shows the typical two-dimensional layered MBene structure, with an irregular flake-like substrate and obvious interlayer wrinkles and cracks, providing abundant sites for Pt nanoparticle loading. Many spherical Pt nanocrystals with uniform size and regular morphology are uniformly dispersed on the support surface. The particles show no obvious agglomeration and are tightly attached to the support surface and interlayer gaps, achieving good dispersion, and providing sufficient active sites for the electrocatalytic reaction. This image directly verifies that Pt nanoparticles are successfully loaded on the MoB support, which is consistent with the XRD phase analysis results, providing direct evidence at the microscopic morphology level for the successful preparation of the Pt/MoB catalyst.

To further analyze the elemental composition and chemical states of Pt/MoB, XPS measurements were performed. The full survey spectrum confirms the presence of Pt, Mo, and O, with no Al signal, indicating successful removal of the Al layer. The B 1s spectrum shows dominant B–Mo bonds, with minor B–O species from slight surface oxidation. The Mo 3d spectrum reveals Mo–B as the main state, with only weak Mo^{4+} signals, demonstrating high structural stability of MoB.for Pt 4f, most Pt exists as metallic Pt^0, with only a small amount of Pt^{2+} from incomplete reduction. The negative shift of Pt^0 binding energy and positive shift of Mo 3d confirm strong metal-support interaction between Pt and MoB, which optimizes the d-band center of Pt, regulates intermediate adsorption, and thus enhances electrocatalytic performance. The high proportion of metallic Pt also significantly improves Pt atomic utilization.

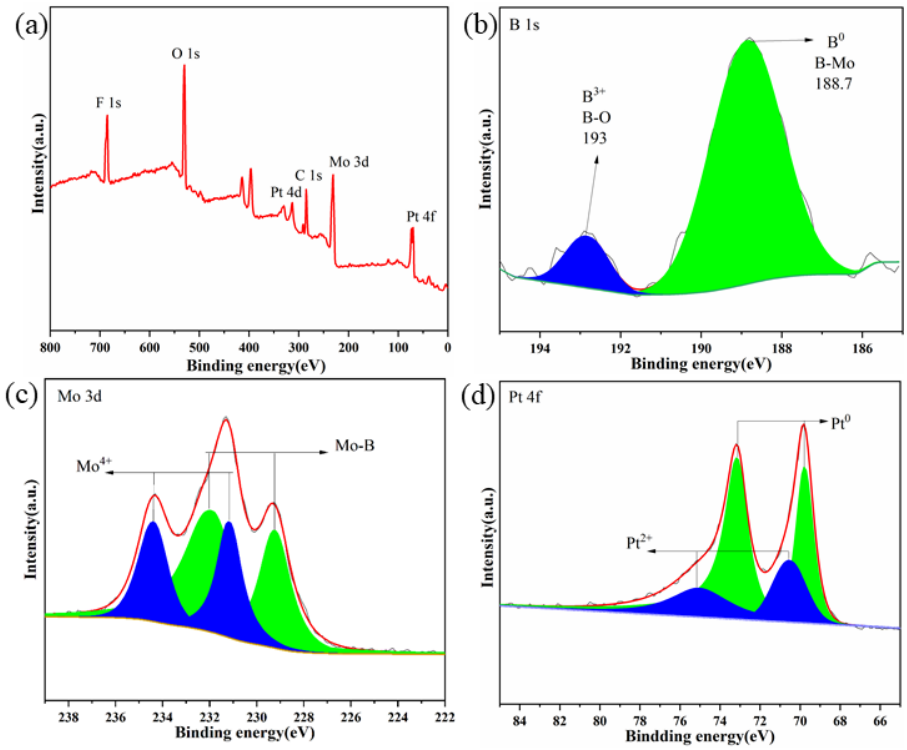

Figure 4 (a) XPS Survey Spectrum of Pt/MoB; High-Resolution XPS Spectra of (b) B 1s, (c) Mo 3d, and (d) Pt 4f for Pt/MoB

B. Electrocatalytic Analysis

The as-prepared Pt/MoB, Pt/Mo_2 C, and commercial Pt/C materials were fabricated into working electrodes. Electrochemical measurements were performed in 0.5 M H_2SO_4 solution using a saturated calomel electrode (SCE) as the reference electrode and a graphite rod as the counter electrode. The test voltage range was set from -0.4 to 0 V with a scan rate of 5 mV·s^{-1}, and the results are presented in Figure 5. Figure 5(a) shows the polarization curves of Pt/MoB, Pt/Mo_2C, and commercial Pt/C in 0.5 M H_2SO_4. At a current density of -10 mA·cm^{-2}, the overpotentials of Pt/MoB, Pt/Mo_2C, and commercial Pt/C are approximately 69 mV, 74 mV, and 39 mV, respectively. This indicates that commercial Pt/C exhibits the lowest overpotential at -10 mA·cm^{-2}, while Pt/MoB and Pt/Mo_2C show similar overpotentials. Although their current density responses to potential are comparable, both are still inferior to Pt/C, preliminarily demonstrating the potential of MoB as a catalyst support.

Figure 5(b) displays the Tafel slopes of Pt/MoB, Pt/Mo_2C, and commercial Pt/C. The commercial Pt/C shows the smallest Tafel slope of 17 mV·dec^{-1}, while Pt/MoB and Pt/Mo_2C exhibit very close Tafel slopes of 27 mV·dec^{-1} and 30 mV·dec^{-1}, respectively, which are consistent with the LSV results. These results reveal that although the HER performance of Pt/MoB and Pt/Mo_2C is not as good as that of commercial Pt/C, they still show excellent catalytic activity. This indicates that both MoB and Mo_2C supports exert favorable electronic modulation or synergistic effects on Pt, and further confirms that MoB, as a novel catalyst support material, is worthy of further investigation.

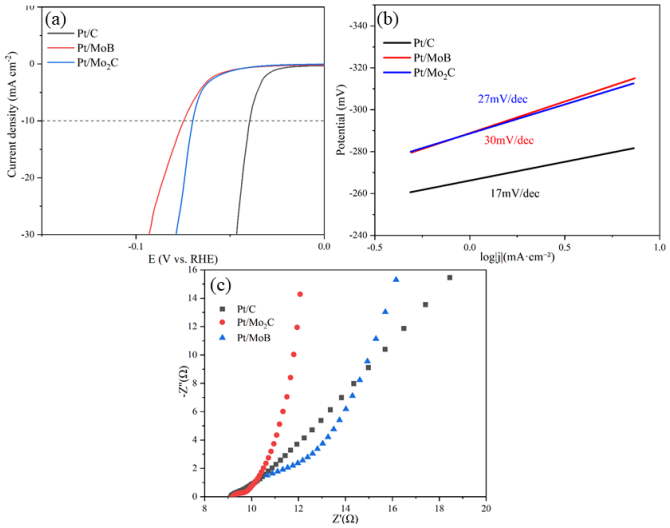

Figure 5 Electrocatalytic Hydrogen Evolution Reaction (HER) Performance Tests of Pt/MoB, Pt/Mo_2C, and Commercial Pt/C in 0.5 mol/L H_2SO_4 Solution: (a) Polarization Curves; (b) Tafel Slopes; (c) Electrochemical Impedance Spectroscopy (EIS) Curves

As shown in Figure 6(c), among all catalysts, commercial Pt/C exhibits the smallest R_{ct} of 4.5 Ω, followed by Pt/Mo_2 C with 6.5 Ω, while Pt/MoB shows the largest R_{ct} of 9 Ω. This indicates that electron transfer in Pt/MoB is relatively difficult, which explains why Pt/MoB shows inferior performance to Pt/Mo_2 C in the LSV curves: the higher electron transfer resistance of Pt/MoB leads to slower reaction kinetics.

To elucidate the intrinsic catalytic activity of Pt/MoB, we measured the electrochemical double-layer capacitance (C_{dl}) and electrochemical active surface area (ECSA) of commercial Pt/C, Pt/Mo_2C, and Pt/MoB catalysts using cyclic voltammetry, as shown in Figure 6. Figure 6 show the current density versus potential curves obtained at different scan rates for Mo_2CT_x, Ru/Mo_2CT_x, and commercial Pt/C. By taking the current density difference (Δj) at the intermediate potential and plotting it against the scan rate, the corresponding C_{dl} values can be determined.

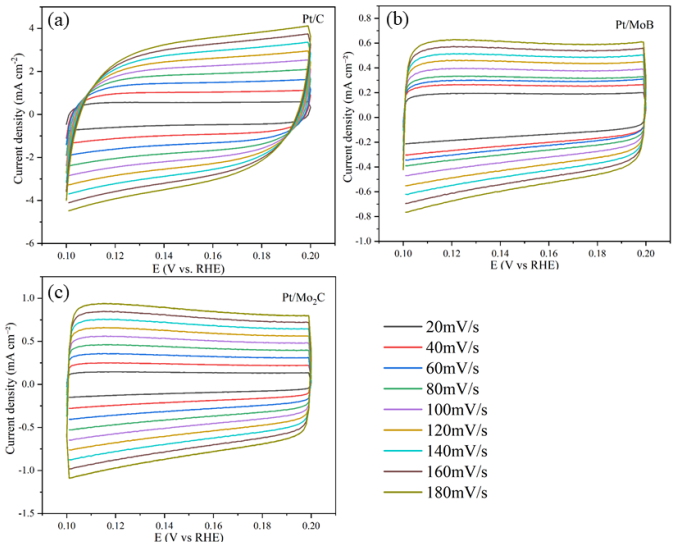

Figure 6 Cyclic Voltammetry Curves of Pt/MoB, Pt/Mo_2 C, and Commercial Pt/C in 0.5 mol/L H_2 SO_4 Solution: (a) Commercial Pt/C; (b) Pt/MoB; (c) Pt/Mo_2 C

Figure 7 shows the Cdl values of different catalysts.It can be observed that the C_{dl} value of Pt/MoB, Pt/Mo_2 C, and commercial Pt/C are 5.17 mF·cm^{-2}, 9.01 mF·cm^{-2}, and 14.9 mF·cm^{-2}, respectively. Pt/C exhibits the highest value, followed by Pt/Mo_2 C, and Pt/MoB shows the lowest. This result also indicates that Pt/MoB has the fewest active sites, which is attributed to the low specific surface area of the MoB support itself and the relatively large size of Pt particles dispersed on MoB, further suggesting that the etching preparation of MoB requires further optimization.

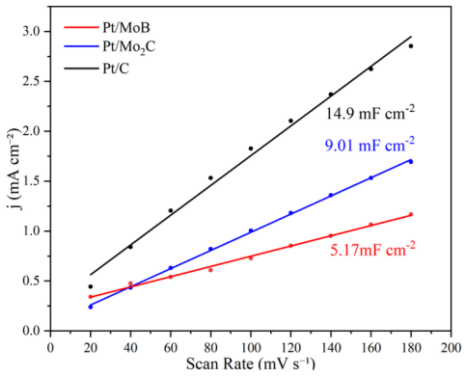

Figure 7 Electrochemical double-layer capacitance curves of Pt/MoB, Pt/Mo_2C, and commercial Pt/C in 0.5 mol/L H_2SO_4 solution

The stability of a catalyst is also a critical performance indicator for practical applications. Therefore, multiple methods were employed to evaluate the stability of the prepared catalyst. Figure 8(a–c) shows the polarization curves before and after 1000 cyclic voltammetry cycles. The polarization curves of Pt/MoB almost overlap completely before and after the cycles, indicating negligible degradation of the HER performance after 1000 cycles and demonstrating excellent electrochemical stability. At the same current density, the overpotential (η) remains nearly unchanged, suggesting that the intrinsic activity and structure of the catalyst are well preserved during cycling. These results confirm that the material exhibits outstanding corrosion resistance and anti-leaching capability in acidic electrolytes.

To further verify the stability of Pt/MoB, chronoamperometry (CA) measurements were performed at a constant potential of 0.5 V, and the corresponding curves are presented in Figure 8(d). The results show no significant decay or fluctuation in the current over 3000 s, indicating that Pt/MoB maintains good electrocatalytic hydrogen evolution performance throughout the test period, which is consistent with the conclusions above.

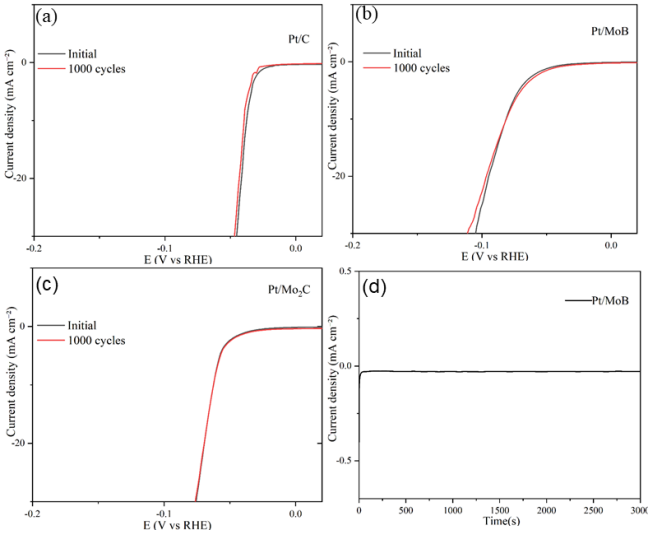

Figure 8 (a–c) Polarization curves of Pt/MoB, Pt/Mo_2C, and Commercial Pt/C Before and After 1000 Cycles in 0.5 mol/L

H_2SO_4 Solution; (d) Chronoamperometric Curve of Pt/MoB at a Constant Potential of 0.5 V

CONCLUTION

In this work, we developed a high-performance Pt/MoB electrocatalyst for the hydrogen evolution reaction (HER) in acidic media by anchoring Pt nanoparticles on MoB supports. The Pt/MoB catalyst exhibits excellent electrocatalytic HER performance, with a low overpotential and fast reaction kinetics, as well as good stability under working conditions.

Systematic characterizations confirmed that the Pt nanoparticles are well-dispersed on the MoB support. The strong metal-support interaction between Pt and MoB leads to optimized electronic structure of Pt, which enhances the adsorption of key HER intermediates. Electrochemical tests show that Pt/MoB exhibits HER activity comparable to Pt/Mo_2C, while the charge transfer resistance and double-layer capacitance measurements indicate that the electronic conductivity and electrochemically active surface area of Pt/MoB are lower than those of Pt/Mo_2C and commercial Pt/C, which can be attributed to the relatively low specific surface area of MoB.

Accelerated stability tests by cyclic voltammetry and chronoamperometry demonstrate that Pt/MoB maintains its activity after long-term operation, confirming its good electrochemical stability. Overall, this work provides a new strategy for designing efficient and stable Pt-based HER electrocatalysts supported on transition metal borides.

References

[1] R. Deng, M. Guo, C. Wang, Q. Zhang, Recent advances in cobalt phosphide-based materials for electrocatalytic water splitting: From catalytic mechanism and synthesis method to optimization design, Nano, Mater. Sci. 6 (2) (2024) 139–173.

[2] B. Jia, B. Zhang, Z. Cai, X. Yang, L. Li, L. Guo, Construction of amorphous/crystalline heterointerfaces for enhanced electrochemical processes, eScience 3 (2)(2023) 100112.

[3] H. Liu, J. Li, J. Arbiol, B. Yang, P. Tang, Catalytic reactivity descriptors of metal nitrogen-doped carbon catalysts for electrocatalysis, EcoEnergy 1 (1) (2023)154–185.

[4] Y. Mu, X. Pei, Y. Zhao, X. Dong, Z. Kou, M. Cui, C. Meng, Y. Zhang, In situ confinedvertical growth of $Co_{2.5}Ni_{0.5}Si_2O_5(OH)_4$ nanoarrays on rGO for an efficient oxygen evolution reaction, Nano, Mater. Sci. 5 (4) (2023) 351–360.

[5] M.S.A. Sher Shah, G.Y. Jang, K. Zhang, J.H. Park, Transition metal carbide-based nanostructures for electrochemical hydrogen and oxygen evolution reactions,EcoEnergy 1 (2) (2023) 344–374.

[6] J. Sun, N. Guo, T. Song, Y.-R. Hao, J. Sun, H. Xue, Q. Wang, Revealing the interfacial electron modulation effect of CoFe alloys with CoC encapsulated in N-doped CNTs for superior oxygen reduction, Adv. Powder Mater. 1 (3) (2022)100023.

[7] Y. Wang, W. Yu, C. Wang, F. Chen, T. Ma, H. Huang, Defects in photoreduction reactions: Fundamentals, classification, and catalytic energy conversion, eScience 4(3) (2024) 100228.

[8] N. You, S. Cao, M. Huang, X. Fan, K. Shi, H. Huang, Z. Chen, Z. Yang, W. Zhang,Constructing P-$CoMoO_4$@NiCoP heterostructure nanoarrays on Ni foam as efficientbifunctional electrocatalysts for overall water splitting, Nano, Mater. Sci. 5 (3)(2023) 278–286.

[9] M. Chen, N. Kitiphatpiboon, C. Feng, A. Abudula, Y. Ma, G. Guan, Recent progress in transition-metal-oxide-based electrocatalysts for the oxygen evolution reaction in natural seawater splitting: A critical review, eScience 3 (2) (2023) 100111.

[10] Y. Gu, N. Nie, J. Liu, Y. Yang, L. Zhao, Z. Lv, Q. Zhang, J. Lai, Enriching H_2O through boron nitride as a support to promote hydrogen evolution from non-filtered seawater, EcoEnergy 1 (2) (2023) 405–413.

[11] L. Hou, H. Jang, X. Gu, X. Cui, J. Tang, J. Cho, X. Liu, Design strategies of ruthenium-based materials toward alkaline hydrogen evolution reaction, EcoEnergy 1 (1) (2023) 16–44.

[12] X. Hu, Y. Li, X. Wei, L. Wang, H. She, J. Huang, Q. Wang, Preparation of double-layered Co−Ci/NiFeOOH co-catalyst for highly meliorated PEC performance in water splitting, Adv. Powder Mater. 1 (3) (2022) 100024.

[13] M. Ma, L. Shen, Z. Zhao, P. Guo, J. Liu, B. Xu, Z. Zhang, Y. Zhang, L. Zhao, Z. Wang,Activation methods and underlying performance boosting mechanisms within fuel cell catalyst layer, eScience (2024) 100254.

[14] J. Li, S. Yan, M. Du, J. Zhang, N. Wu, G. Liu, H. Chen, C. Yuan, A. Qin, X. Liu, The impact of support electronegativity on the electrochemical properties of platinum,J. Colloid Interface Sci. 662 (2024) 183–191.

[15] J. Li, N. Wu, J. Zhang, H.-H. Wu, K. Pan, Y. Wang, G. Liu, X. Liu, Z. Yao, Q. Zhang,Machine Learning-Assisted Low-Dimensional Electrocatalysts Design for Hydrogen Evolution Reaction, Nano-Micro Letters 15 (1) (2023) 227.

[16] P. Liu, X. Zhang, J. Fei, Y. Shi, J. Zhu, D. Zhang, L. Zhao, L. Wang, J. Lai, Frank Partial Dislocations in Coplanar Ir/C Ultrathin Nanosheets Boost Hydrogen Evolution Reaction, Adv. Mater. 36 (11) (2023) 2310591.

[17] S. Pan, C. Li, T. Xiong, Y. Xie, F. Luo, Z. Yang, Hydrogen spillover in MoOxRh hierarchical nanosheets boosts alkaline HER catalytic activity, Appl. Catal. B Environ. Energy 341 (2024) 123275.

[18] J. Yan, R. Wu, G. Jin, L. Jia, G. Feng, X. Tong, The hybrid Pt nanoclusters/Ru nanowires catalysts accelerating alkaline hydrogen evolution reaction, Adv.Powder Mater. 3 (5) (2024) 100214.

[19] L. Yang, R. Grzeschik, P. Jiang, L. Yu, C. Hu, A. Du, S. Schlücker, W. Xie, Tuning the Electronic Properties of Platinum in Hybrid-Nanoparticle Assemblies for use in Hydrogen Evolution Reaction, Angew. Chem. Int. Ed. 62 (25) (2023) e202301065.

[20] L. Zhao, J. Jiang, S. Xiao, Z. Li, J. Wang, X. Wei, Q. Kong, J.S. Chen, R. Wu, PtZn nanoparticles supported on porous nitrogen-doped carbon nanofibers as highly stable electrocatalysts for oxygen reduction reaction, Nano, Mater. Sci. 5 (3)(2023) 329–334.

[21] Z. Li, R. Ge, J. Su, L. Chen, Recent Progress in Low Pt Content Electrocatalysts for Hydrogen Evolution Reaction, Adv. Mater. Interfaces 7 (14) (2020) 2000396.

[22] L.Y. Zhang, T. Zeng, L. Zheng, Y. Wang, W. Yuan, M. Niu, C.X. Guo, D. Cao, C.M. Li,Epitaxial growth of Pt–Pd bimetallic heterostructures for the oxygen reduction reaction, Adv. Powder Mater. 2 (4) (2023) 100131.

[23] S. Lakshmy, B. Mondal, N. Kalarikkal, C.S. Rout, B. Chakraborty, Recent developments in synthesis, properties, and applications of 2D Janus MoSSe and MoSex S(1–x) alloys, Adv. Powder Mater. 3 (4) (2024) 100204.

[24] X. Zhang, F. Jia, S. Song, Recent advances in structural engineering of molybdenum disulfide for electrocatalytic hydrogen evolution reaction, Chem. Eng. J. 405(2021) 127013.

[25] M. Miao, J. Pan, T. He, Y. Yan, B.Y. Xia, X. Wang, Molybdenum Carbide-Based Electrocatalysts for Hydrogen Evolution Reaction, Chem. Eur. J. 23 (46) (2017)10947–10961.

[26] R.A. Mir, S. Upadhyay, O.P. Pandey, A review on recent advances and progress in Mo2C@C: A suitable and stable electrocatalyst for HER, Int. J. Hydrogen Energy 48(35) (2023) 13044–13067.

[27] R. Ge, J. Huo, T. Liao, Y. Liu, M. Zhu, Y. Li, J. Zhang, W. Li, Hierarchical molybdenum phosphide coupled with carbon as a whole pH-range electrocatalyst for hydrogen evolution reaction, Appl. Catal. B Environ. Energy 260 (2020)118196.

[28] Y. Gu, A. Wu, Y. Jiao, H. Zheng, X. Wang, Y. Xie, L. Wang, C. Tian, H. Fu, Two-Dimensional Porous Molybdenum Phosphide/Nitride Heterojunction Nanosheets for pH-Universal Hydrogen Evolution Reaction, Angew. Chem. Int. Ed. 60 (12)(2021) 6673–6681.

[29] H. Chen, X. Zou, Intermetallic borides: structures, synthesis and applications in electrocatalysis, Inorg. Chem. Front. 7 (11) (2020) 2248–2264.

[30] F. Guo, Y. Wu, X. Ai, H. Chen, G.D. Li, W. Chen, X. Zou, A class of metal diboride electrocatalysts synthesized by a molten salt-assisted reaction for the hydrogen evolution reaction, Chem. Commun. 55 (59) (2019) 8627–8630.

[31] X. Wang, G. Tai, Z. Wu, T. Hu, R. Wang, Ultrathin molybdenum boride films forhighly efficient catalysis of the hydrogen evolution reaction, J. Mater. Chem. A 5(45) (2017) 23471–23475.

[32] K.J. Baumler, L.T. Alameda, R.R. Katzbaer, S.K. O'Boyle, R.W. Lord, R.E. Schaak,Introducing Porosity into Refractory Molybdenum Boride through Controlled Decomposition of a Metastable Mo–Al–B Precursor, J. Am. Chem. Soc. 145 (2)(2023) 1423–1432.

[33] H. Vrubel, X. Hu, Molybdenum Boride and Carbide Catalyze Hydrogen Evolution in both Acidic and Basic Solutions, Angew. Chem. Int. Ed. 51 (51) (2012)12703–12706.

[34] C.S. Rout, P.V. Shinde, A. Patra, S.M. Jeong, Recent Developments and Future Perspectives of Molybdenum Borides and MBenes, Adv. Sci. 11 (21) (2024)2308178.